Solid Freeform Fabrication 2022: Proceedings of the 33rd Annual International Solid Freeform Fabrication Symposium – An Additive Manufacturing Conference
Reviewed Paper

Utilizing Lattice Infill Structures to Optimize Weight with Structural Integrity Investigation for Commonly Used 3D Printing Technologies

Mohammad Alshaikh Ali[Ψ], Ismail Fidan[Ψ], Michael Allen[Ψ],
Indranil Bhattacharya[Ψ], and Khalid Tantawi[β]

[Ψ]Tennessee Tech University
Cookeville, TN 38505

[β]University of Tennessee at Chattanooga
Chattanooga, TN 37403

Abstract

Additive Manufacturing (AM) is utilized in various applications and fields. This research study investigates the use of lattice infill structures to reduce weight in two commonly used AM methods; Stereolithography (SLA) and Fused Filament Fabrication (FFF). Structural integrity of lattice infilled parts is investigated. Before utilizing lattice infill structures, different process parameters are also investigated to gain a knowledge base for these patterns' effect on weight and power consumption (PC). Cubes are used as test specimens to perform the knowledge base study for the process parameters. Based on the initial study, an infill pattern is chosen to be compared with a lattice infill structure. The test specimens for this study are chosen to be of different background and complexity. Experimental data indicates a reduction in weight with no increase in PC for SLA and an increase in PC for FFF. Lattice infilled structures respond well to structural integrity testing.

Keywords: Additive Manufacturing, Stereolithography, Fused Filament Fabrication, Lattice Structure, Energy Consumption

Introduction

Industries are utilizing AM technologies now more than ever. The main reason being that AM technologies are capable of manufacturing artifacts that other manufacturing processes cannot. With that said, AM technologies have revolutionized the manufacturing industry. With more advancements in the development of AM technologies, the trend of industries shifting to AM is just the beginning. While there are several different AM technologies, this research focuses on Fused Filament Fabrication (FFF) and Stereolithography (SLA), shown in Figure 1.

One of the most commonly used AM technologies is FFF, also known as Material Extrusion. This technology is used by various industries, small businesses, and hobbyists. The

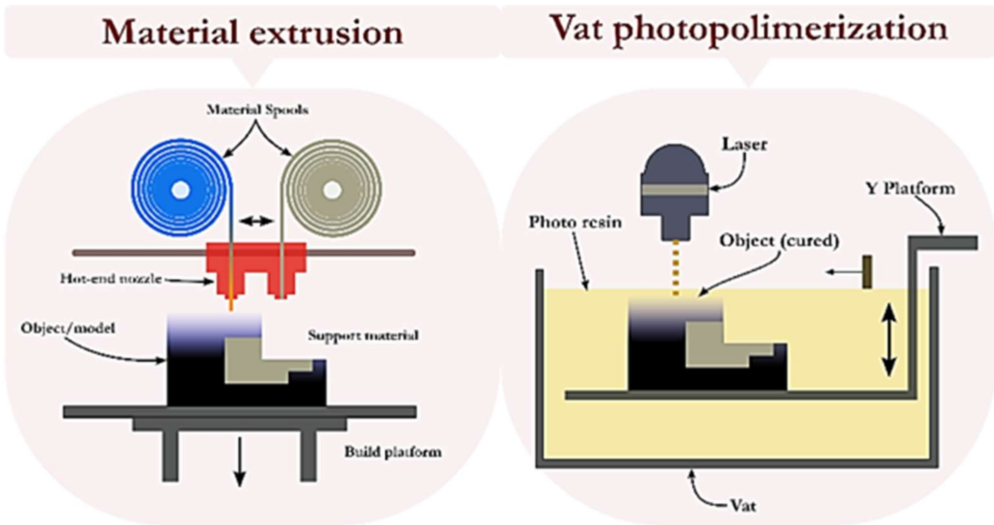

Figure 1: Material Extrusion (FFF) and Vat Photopolymerization (SLA) processes shown in more detail [1]

technology involves melted polymers deposited layer-by-layer until the desired object is formed. The polymer is typically extruded through a nozzle by a gear mounted on an electric motor. The material is extruded on a build platform that is often heated to help with adhesion and reduce warping. The desired object can be acquired by Computer Aided Design (CAD) [2] modeling or from online sources. The CAD file is converted to an STL file to be imported into FFF pre-processing.

Pre-processing of models for FFF involves a process called slicing. This process is where all the manufacturing parameters are set, like extrusion temperatures, speeds, infill patterns, infill density, and many others. The infill pattern dictates the internal structure type in the model. Infill density on the other hand, dictates how often the infill structure is repeated. These parameters contribute highly to shape the fabrication of the model. They also affect the mechanical and physical characteristics of the fabricated model. In addition, these parameters affect the operating energy usage of the fabrication process.

Another widely used AM technology is SLA, also known as Vat Photopolymerization. This technology utilizes photo-sensitive resin combined with a light-source, like a laser, to form the model desired. The build plate of the SLA machine gets submerged with the resin enough to form a layer, followed by solidification of said resin using a light source. The build platform must be enclosed by UV resistant material, in order to prevent the resin from curing and solidifying. Like FFF, pre-processing must be performed to the STL file.

SLA pre-processing also involves slicing; most process parameters, however, are different than those of FFF. An example process parameter for SLA fabrication would be layer height, which is the thickness of each layer solidified. Unlike FFF, SLA models almost always require post-processing to get beneficial characteristics out of a part. Post-processing often includes removal of support structures, washing, and curing. Washing is typically done with Isopropyl

Alcohol to clean the part. After, curing is performed to strengthen the part and solidify any uncured resin leftover from fabrication and washing.

With these technologies being utilized more comfortably, more advanced parameters and techniques are being developed and explored. Several light-weighting tools are being explored and investigated for additively manufactured parts. Some of these tools are Topology Optimization, Generative Design, and using lattice infill structures, or patterns, instead of typical infill patterns such as lines, triangles, gyroid, and several others.

Studies have shown that these two AM technologies have high capabilities considering their relatively low cost, i.e. compared to injection molding.. They do, however, have advantages and disadvantages for different applications. For example, SLA is superior when it comes to intricate details and surface finish, while FFF can typically fabricate faster than SLA. While several benchmarking studies have been done to compare several AM technologies, there is always room and use for research that provides a knowledge base to vital operating variables. Table 1 includes some of the benchmark research that is done for SLA and FFF processes, preceded by brief summaries of a few research studies.

Kim et. al [3] introduced several AM technologies, like FFF, SLA, poly-jet, and Selective Laser Sintering. The authors' aim was to benchmark the mentioned AM technologies by exploring their mechanical properties, geometrical accuracy, surface roughness, speed, and cost of materials. Parts are printed for experimentation for each property tested or measured. Their results indicate that impact and tensile strength is highly dependent on the printing direction. For dimensional accuracy, SLA proved to be the most accurate and lowest surface roughness.

Jayaram et. al [4] investigated a few different AM technologies: SLA, SLS, Laminated Object Manufacturing (LOM), and FFF. A test artifact is designed to have various features (sharp tips, tilts, etc.) and later be tested. Results indicated that SLA was the most aesthetic AM process compared to all the others, considering SLA had all the intricate features fabricated with the lowest surface roughness. All AM technologies were able to produce their design with SLA being the only technology able to achieve a sharp-as-designed tip. The authors stated all processes had disadvantages when it comes the materials used like temperature control requirements for SLS, time-delay requirements for SLA, and stringing in the FFF process. Post-processing of produced parts is addressed as well; stating FFF parts requires the least post-processing followed by SLS and SLA in respective order.

Choudhari et. al [5] explored the benchmarking of a few different AM processes as well, SLA, SLS, and FFF with respect to properties and parameters like build time, surface finish, cost, and shrinkage rate. The authors stated that SLA-produced part displayed the least shrinkage and the best surface finish compared to SLS and FFF produced parts. It was also found that FFF would be ideal for low-cost low-accuracy production, as the material (ABS) they used in FFF is cheaper than the materials used in the other processes.

Terry et. al [6] reviewed different aspects of Smart Manufacturing (SM), which includes AM. They focus on the advantages of energy saving and production efficiency. Their review paper explains the advantages of utilizing SM for energy saving and efficiency. They also point out areas that SM could be further explored to improve employment of SM in industries.

Hinshaw et. al [7] developed a knowledge base to explore some process parameters and energy consumption of FFF AM technology. The process parameters the authors explored are layer height, infill density, and side shells. Their results indicate that the highest layer height of .3mm with 25% infill and 3 side shells consumed the least energy.

Chu et. al [8] explored the use of a cubic lattice infill pattern to decrease material usage. The lattice infill is compared to traditional infill patterns. The test specimens' weight is simulated using slicing software. The result of that simulation indicates a reduction of material use of up to 63%. In addition, stress simulation is used to investigate the structural integrity of the test specimen. Simulation results indicate the lattice-filled cube can sustain a compressive load of up to 1.6 kN.

Initial Parametric Study

The objective of this parametric study is to establish a knowledge base for how some process parameters affect a few different response variables. The data gathered from this study is later used for a validation study that also introduces a cubic lattice infill structure. The process parameters are layer height (LH), infill pattern (IP), and infill density (ID). For each process parameter, three levels are chosen in order to establish a 3x3 factorial design. The process parameter levels are shown in Table 2. The response variables investigated are power consumption (PC), mass, and surface roughness (SR). The test specimens used are 0.5 inch cubes.

FFF and SLA Setup

The general procedure for this study is shown in Figure 2. Cubes are designed in CAD software and exported as an STL file to be used as test specimens, Typically, slicing software is

Table 1: Literature Review for Benchmarking SLA and FFF Processes

Author	Year	Finding(s)	Reference #
Kim et. al	2007	Mechanical properties, geometrical accuracy, surface roughness, speed, cost	[3]
Jayaram et. al	1994	Dimensional accuracy, part-processing requirements	[4]
Mahesh et. al	2005	Decision-making system development	[9]
Choudhari et. al	2016	Build time, surface finish, cost, shrinkage	[5]
Johnson et. al	2014	Surface roughness vs layer height	[10]
Rebaioli	2017	Review on benchmarking artifacts	[11]
Chu et. al	2020	Material efficiency using lattice infill structure	[8]
García-Domínguez et. al	2019	Infill optimization technique development	[12]

Table 2: Parametric Study Process Parameters

Process Parameter	**Values**		
Layer Height (mm)	0.025	0.05	0.1
Infill Density (%)	10	20	30
Infill pattern	Lines	Triangles	Hex
Note: this table shows the process parameters along with the corresponding values or levels.			

used to pre-process the model and directly fabricate. In this research, however, infill patterns are one of the process parameters investigated. Models are usually fully solid in the SLA process, with no infill pattern or variable infill density. For this reason, ANSYS SpaceClaim [13] is used to shell (hollow) and infill the models. In addition, one face of the cube is removed as best practice to not trap unwanted resin in the SLA fabrication process.

For FFF, Raise3D Pro2 [14] machine is used to fabricate the cubic specimens. The slicer most compatible with this machine is ideaMaker [15], which is especially tailored for Raise3D machines.

The material used for this research is generic Polylactic Acid (PLA). As for SLA, a Formlabs Form 2 [16] machine is used, along with Preform [17] slicing software, which is tailored for Formlabs machines. The material used for SLA printing is V4 Clear resin from Formlabs.

Power Logging Setup

While the parts are being fabricated, power data is logged using Watts Up Pro [18] along with their Logger Pro software. The setup consists of a laptop computer, with Logger Pro installed, connected to the power logger, Watts Up Pro. The power logger is connected to a power outlet, and the FFF or SLA machine's power cable is connected to the power logger. For each fabrication process, the machine is allowed to fully cool down before starting the next fabrication process. This ensures the data includes the initiation process for both AM technologies. It should be noted that both 3D printers are in temperature-controlled environments. Within the power logging software, a sampling rate can be set. For this research, a sampling rate of 2 Hz is set, to ensure a full capture of the power data as the specimens are considered small and quick to fabricate.

The logging setup gathers data in terms of power in Watts. To measure the PC, the average power is taken for each specimen and multiplied by the run time. Before this step, however, data post-processing must be performed. Each data file is manually trimmed in order to eliminate any out-of-fabrication data. This is determined by looking at sudden and persistent changes in power. Once this is done, the average power can be taken along with the print time.

Mass and Surface Roughness Measurement Setup

The mass of the cubes is measured using a Mettler Toledo PL-602S [19] weight scale. This weight scale measures with an accuracy of up to a 100th of a gram, since the specimens will potentially only vary within 100th of a gram. The specimens are stripped of all support structures left from fabrication. For SLA, the parts are cured after fabrication and removal of supports.

A Mitutoyo SJ-210 [20] profilometer is used to measure the surface roughness the specimens. For each specimen, the probe of the profilometer is dragged across, or perpendicular to, the layer lines. This is typically how roughness measurements are taken for additively manufactured parts, as the probe has a needle that may be guided by layer lines if dragged along the layer lines, which does not yield desired data.

Parametric Study Results and Analysis

Data collected is analyzed to extract the best parameters for each response variable. This may be different for each AM technology. Statistical Analytics Software (SAS) is used to perform the analysis. A correlation study is performed to guide the decision of using Analysis of Variance (ANOVA) or Multivariate Analysis of Variance (MANOVA). Correlation results lead to using MANOVA, which is performed using SAS. A priori of 0.01 is taken into consideration.

For FFF, MANOVA results indicate all process parameters have main effects on all response variables. This conclusion is drawn because of P-values being lower than the priori. As seen in Table 3, the highest F value corresponds to the layer height process parameter. This indicates that layer height is the most influential process parameter on response variables from the FFF data collected.

Table 3: MANOVA Results

	FFF		**SLA**	
	P Value	**F Value**	**P Value**	**F Value**
Overall IP Effect	<.0001	52.76	.0003	10.96
Overall ID Effect	<.0001	30.88	<.0001	15.65
Overall LH Effect	<.0001	177.56	<.0001	51.10

Note: P values less than 0.01 indicate statistical significance in main effects. Higher F values indicate higher significance.

For SLA, MANOVA results yield to a similar conclusion to FFF's. Where all process parameters have main effects on all response variables. With that said, layer height continues to be the most influential process parameter with an F-value larger than the other process parameters.

Data is plotted to observe the effects of each level of all process parameters, on all response variables. As expected, LH-sorted data yields a non-zero slope linear relationship across the different levels. In other words, different LH levels have significantly different results. For mass, however, LH has minimal effect on SLA produced parts. On lower levels of LH in FFF, mass sees an increase, which is unexpected. It is believed that the reason for this is the machine's inability to regulate flowrate at this small of a LH, as FFF machines typically do not operate on a 0.025 mm LH.

Plots showing ID effects only have major effects on mass, slight effects on PC, and almost no effect on SR. This is expected as well for a few reasons. Logically, mass is heavily dependent on ID; the higher the ID the higher the mass. As for SR, ID only affects what is done internally to the model; unless the walls are thin enough to show infill overlaps, which is rare. More ID means more material is deposited internally, which should result in a higher PC as ID goes up. In this case, however, the infill area is relatively small which is why PC sees a slight increase as ID goes up.

Data for IP shows no apparent effect on SR, which is also expected as IP only affects the model internally. Across the other response variables, the only trend observed is within mass; where Honeycomb IP yields the lightest models and Lines IP yields the heaviest.

SLA vs FFF Data

Table 4 shows that SLA uses 23% of the power that FFF would use for the same parts. In other words, FFF uses four times the power as SLA does. This is a significant difference in averages in power consumption. Looking at Table 4, SLA printed specimens have 72% less surface roughness than those of FFF, on average. This is also a significant difference in surface roughness between the two technologies. Moving on to build time, FFF takes 15% less time than SLA on average. This is not a noticeable difference for this scale of specimens, it could however, be more significant on a larger scale.

Looking at mass data in Table 4, it indicates the material used in FFF is less dense than the resin used in SLA. The resin used has a density between 1.15 and 1.20 g/cm^3, according to the manufacturer. The average density of PLA from many manufacturers is around 1.25 g/cm3. Wall Eye (www.walleyesolutions.com) does not have a data sheet for their PLA material. If mass is calculated using the material densities provided along with the volumetric data provided by slicing software, the results would be different than what is produced and scaled. There could be a few different reasons for this. One potential cause for SLA would be that more resin is solidifying than needed. This could be because of the high viscosity of the resin and its poor draining ability. For FFF, this could be because printing or slicing inaccuracy. Going back to the mass data in the statistical analysis chapter, the mass accuracy of the 0.1 mm layer height is much greater than its

Table 4: Simple Statistics for Response Variables

	Power Consumption (Whr)				**Surface Roughness (microinch)**			
	Mean	Max.	Min.	Std. Dev.	Mean	Max.	Min.	Std. Dev.
FFF	472.37	1122	150.8	250.36	320.159	620.66	155.0	121.3
SLA	109.26	171.7	57.0	42.72	89.64	220.95	52.08	48.001
	Build Time (min)				Mass (g)			
	Mean	Max.	Min.	Std. Dev.	Mean	Max.	Min.	Std. Dev.
FFF	120.987	282.33	38.08	65.208	1.06031	1.61	0.59	.27108
SLA	141.45	227.41	31.42	64.56	1.69926	2.64	1.13	.44754

Note: This data is extracted from SAS results for both SLA and FFF.

counterparts. This is believed to be because of the printer's inability to regulate flow rates at this small of a scale, at 0.025 mm and 0.05 mm LH, with a 0.4 mm nozzle diameter.

Best Process Parameters

The analysis done provides information on what the best process parameters are for good PC, SR, and lightweight. The LH chosen is 0.1 mm; for its lower PC for both FFF and SLA, plus lower mass data for FFF. While this LH level yields higher SR, it is still considered good quality and applicable in many areas. The ID chosen is 10% which yields least mass and least PC, without any effect on SR. The IP chosen is Honeycomb, for its lower mass characteristics and no apparent effect on PC or SR.

Validation Study and Lattice Infill

The previous chapter states the best process parameters for the response variables in mind. The conclusions drawn and the best process parameters are based on cubic specimens. Can the same conclusion be drawn for other specimens? This chapter aims to validate the benchmarking study with three different complex parts, a bolt, a steering knuckle, and a knee joint. In addition to validation, a cubic lattice infill structure, or pattern, is introduced to explore its light-weighting capabilities.

The process parameters chosen for the validation study are slightly different than those idealized in the previous chapter. The only different parameter is ID, which is chosen to be 20% instead of 10%. The reason is that the models are relatively small, and the walls may be the sole affecter instead of the IP. The 20% ID is believed to lead to the full capture of the cubic lattice IP effect.

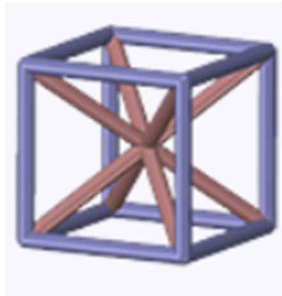

Figure 2: Cubic lattice structure utilized in this experiment

Models

The models, shown in Figure 3, are simply downloaded from Thingiverse (www.thingiverse.com) as STL files. The models are: knee joint [21], steering knuckle [22], and a bolt [23]. The STL files are then modified to have the same overall volume while maintaining the aspect ratio. The models are then imported to Meshmixer in order to add drain holes. Drain holes are added for SLA produced parts, as they need a drainage mechanism for shelled models.

Results and Discussion

The fabricated parts are seen in Figure 4. Looking at Figure 5 and Figure 6, it is seen that across the three models with both infill patterns, SLA only uses around 12.4 percent of the power that FFF uses. In other words, FFF uses 8 times more power than SLA on average. For FFF, lattice infill structures use 9.0% more power than honeycomb infill pattern across the three models. For SLA, the lattice-infilled models consumed only 2.03% more power than the honeycomb-infilled parts.

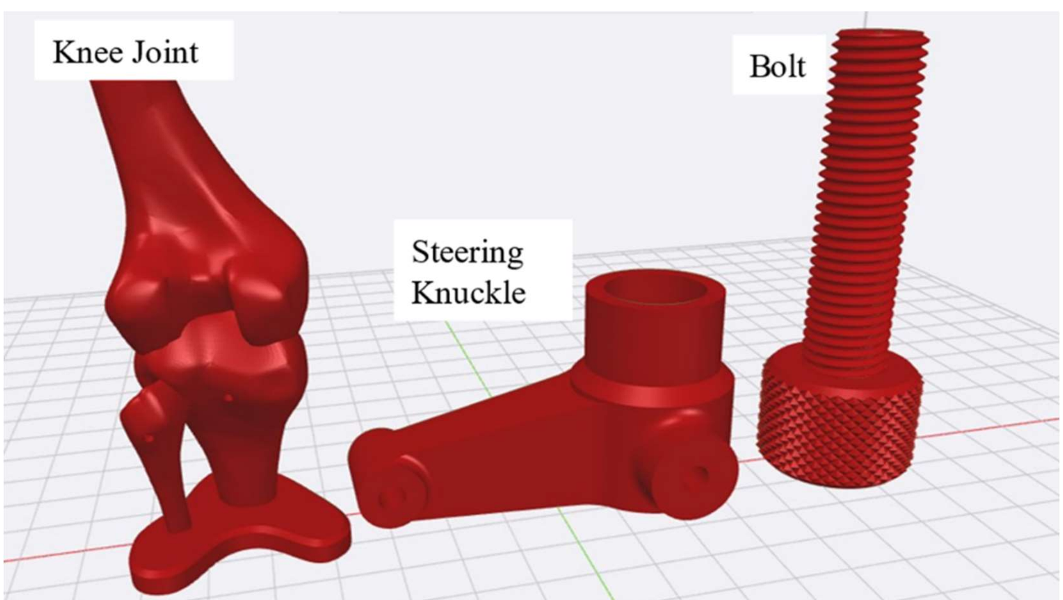

Figure 3: Validation Study Models

Figure 4: Parts fabricated by FFF (left) and SLA (right)

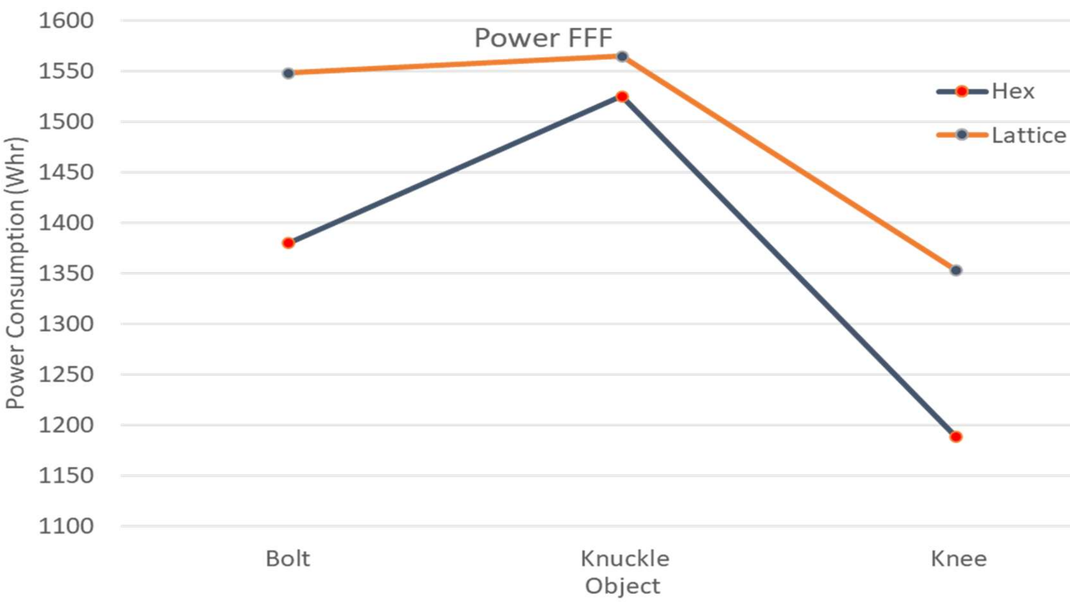

Figure 5: Power Results for Validation Study (FFF)

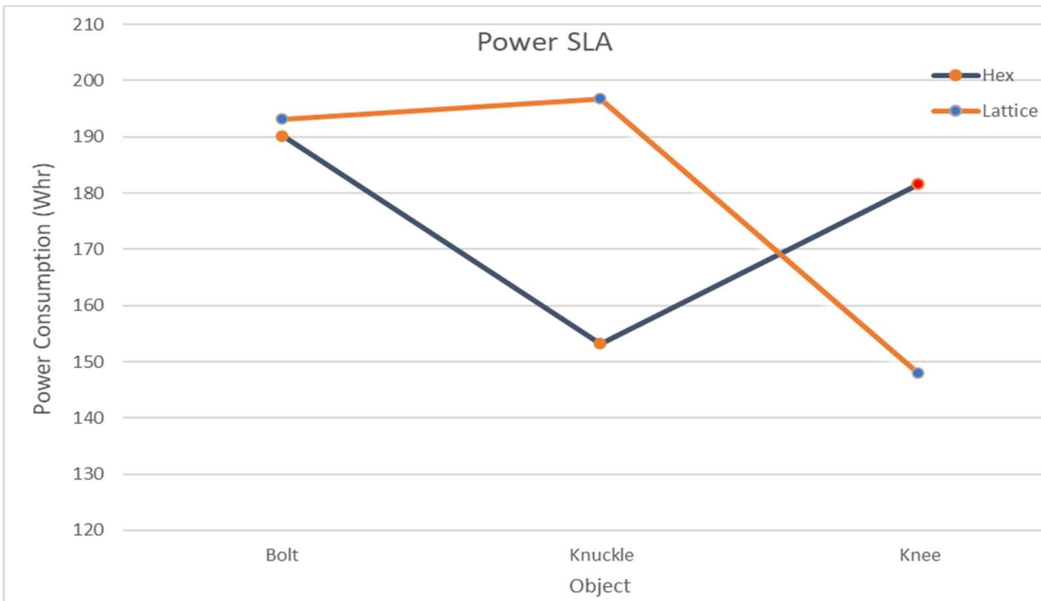

Figure 6: Power Results for Validation Study (SLA)

Looking at the mass plots in Figure 7 and Figure 8, it is seen that the FFF mass plots for the different infill patterns are almost overlapping. The average difference is only 1.5% for all three parts for FFF prints. For SLA, however, lattice-infilled parts are 20.82% lighter than the honeycomb-infilled parts. This is a significant reduction in weight on such a small scale. It is possible however that the honeycomb steering knuckle model performed poorly with resin draining, as it was significantly heavier than its lattice-infilled counterpart. For this reason, another identical model is produced in the same conditions, yielding the same result as the initial sample.

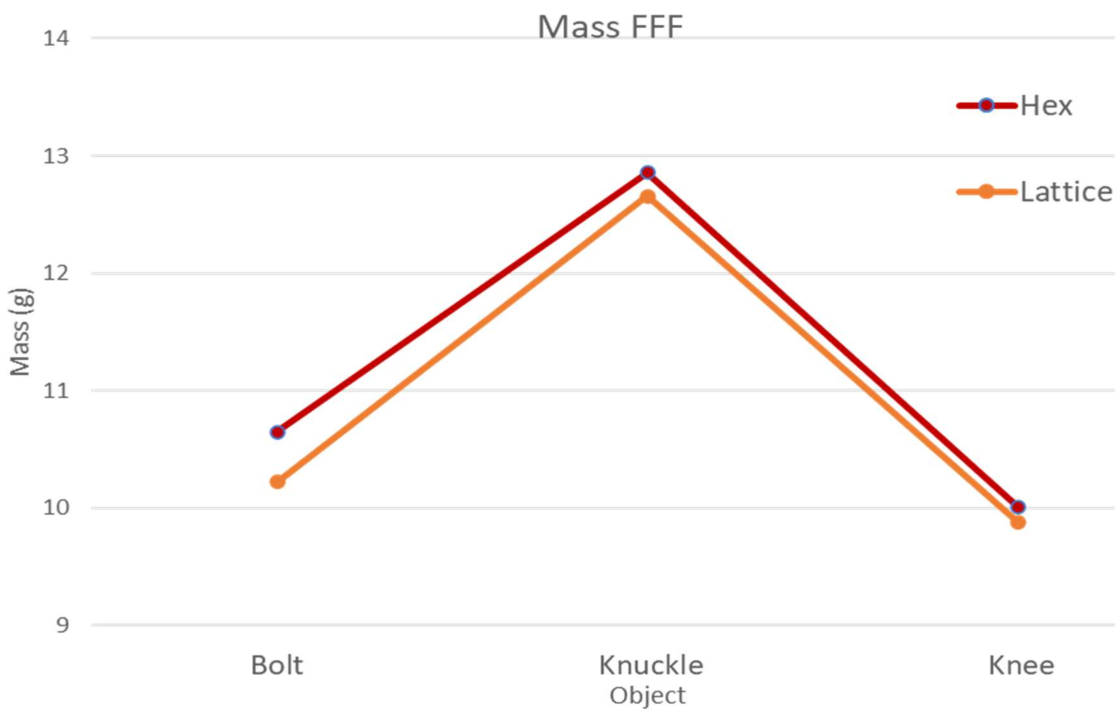

Figure 7: Mass Results for Validation Study (FFF)

Compression Tests

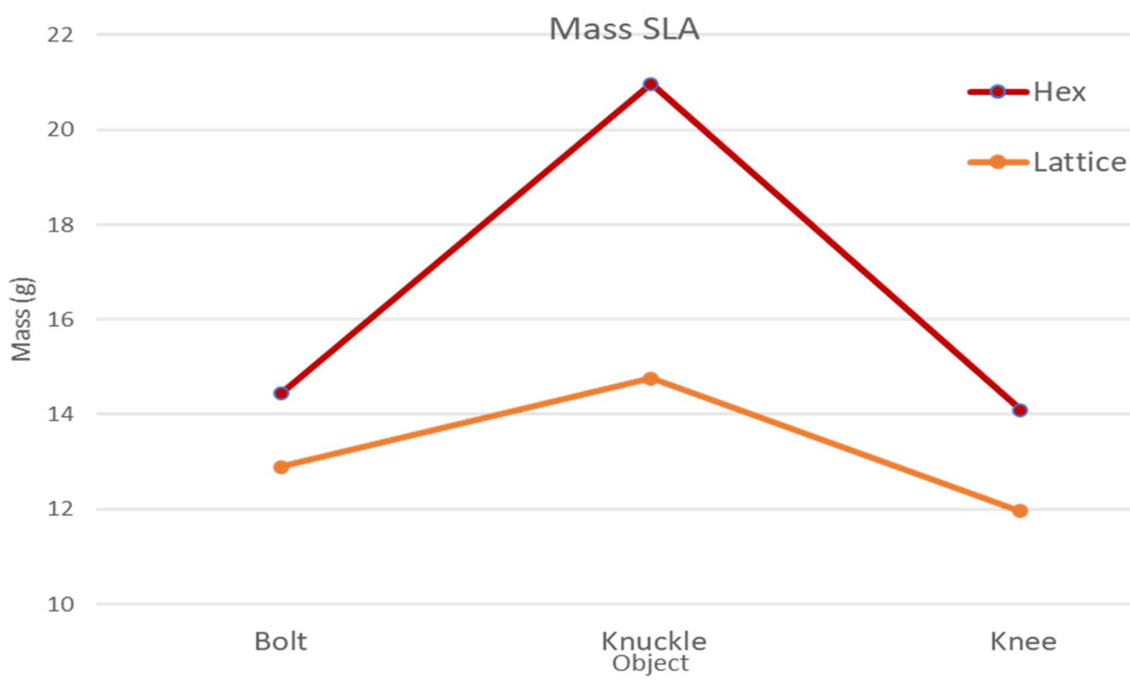

Figure 8: Mass Results for Validation Study (SLA)

The cubic lattice IP does in fact increase material efficiency, but how much structural integrity is sacrificed? This section aims to explore the compressive stress abilities of the material efficient IP for both SLA and FFF. The reason both technologies are explored is because each technology has a different bonding mechanism, which may yield completely different results.

Cylindrical specimens, Figure 9, are designed in CAD and exported as STL files. The dimensions of the cylindrical samples are 30 mm diameter and 30 mm length. In SpaceClaim, the wall thickness is set to 1 mm, in order to reduce effect of walls on the results. To recap, SLA needs a draining mechanism to function properly with shelled models. For this reason, the top and bottom faces are removed, which yields in an excellent draining mechanism. For FFF, the top and bottom faces are left as is at 1 mm thickness.

Compression results indicate that the cubic lattice infill structures can take a decent load before yielding in compression. However, the honeycomb pattern, or hex, is far more superior in taking the same compressive load. From Figure 10, it looks like the two FFF hex specimens reacted differently to the compressive test, as one has a maximum compression yield strength of 1049 psi, while the other has a maximum compression strength of 12473 psi. The FFF lattice specimens are consistent with the results, as one has a maximum compression strength of 5970 psi and the other at 5385 psi. With that said, the lattice structure specimens averaged 49% of the hex specimen's compression strength.

For SLA specimens, Figure 11 displays similar results are seen when it comes to comparing the two infill structures. The maximum compression strength for the two hex specimens are at 13792 and 13933 psi. The lattice infill structure specimens yielded compression strengths of 7254 and 6704 psi. This result yields almost the exact ration when comparing the two infill patterns. As the lattice infill specimens have 50% of the hex-filled specimens.

This is a significant loss in compressive strength with not much reduction in mass. It should be noted however, that the cubic lattice chosen here should behave in a more isotropic nature than the hex would. In other words, if the pattern was directed towards the x or y direction, the specimens would have behaved very differently. For lattice-filled specimens, however, the structure is exactly the same in the other two directions and is ensured to behave the same. The isotropic behavior is how the cubic lattice infill structure would be desired more than the honeycomb for example. Further tests and experimentation are needed for a solid conclusion.

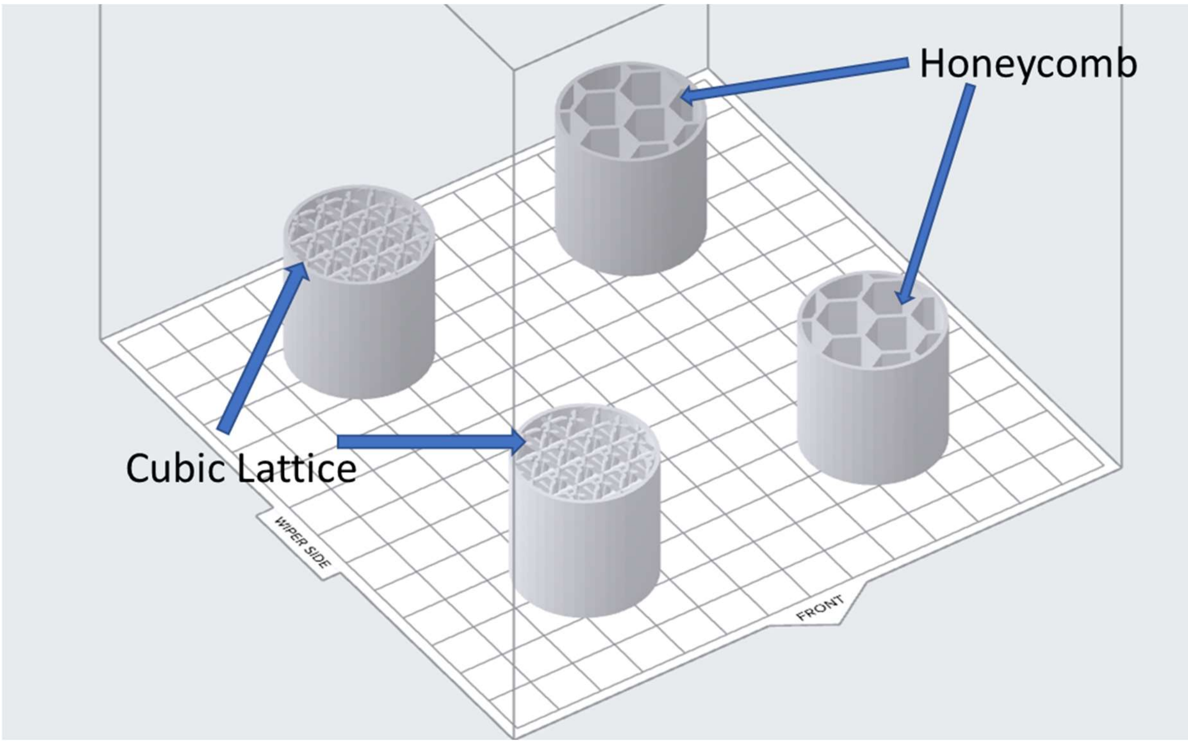

Figure 9: Cylindrical samples used for compression testing

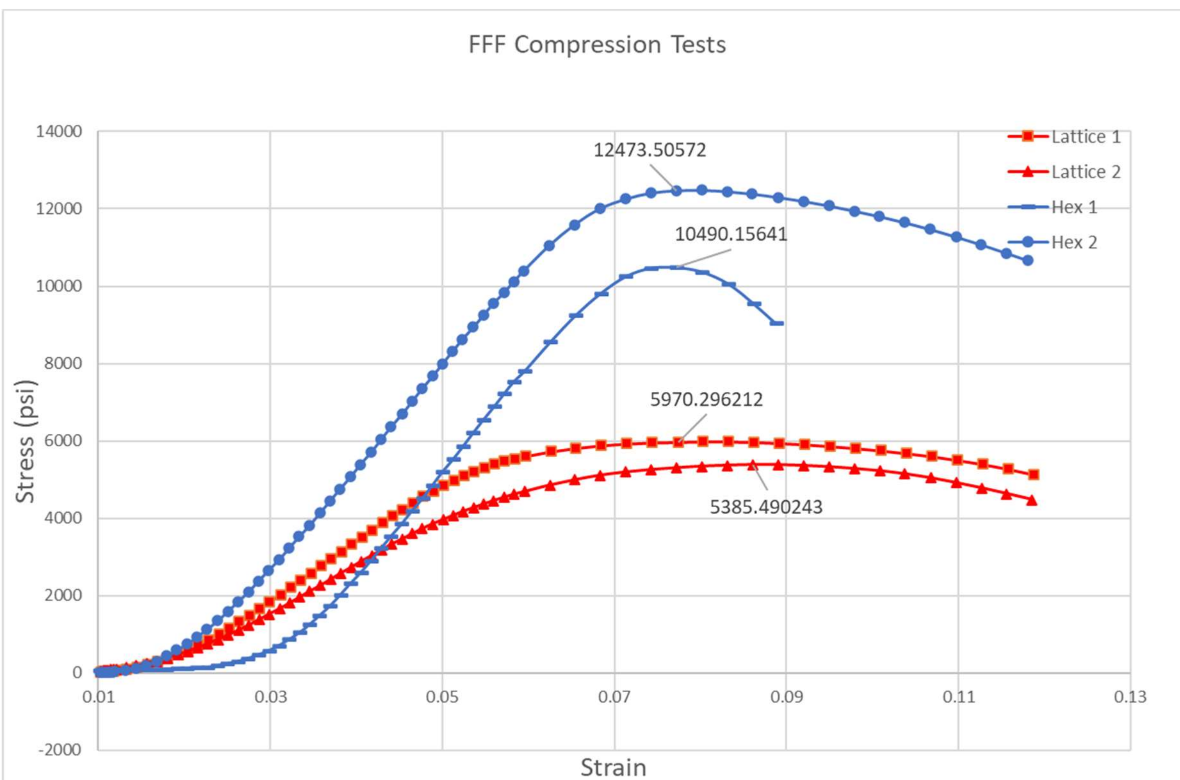

Figure 10: FFF Compression Test Results

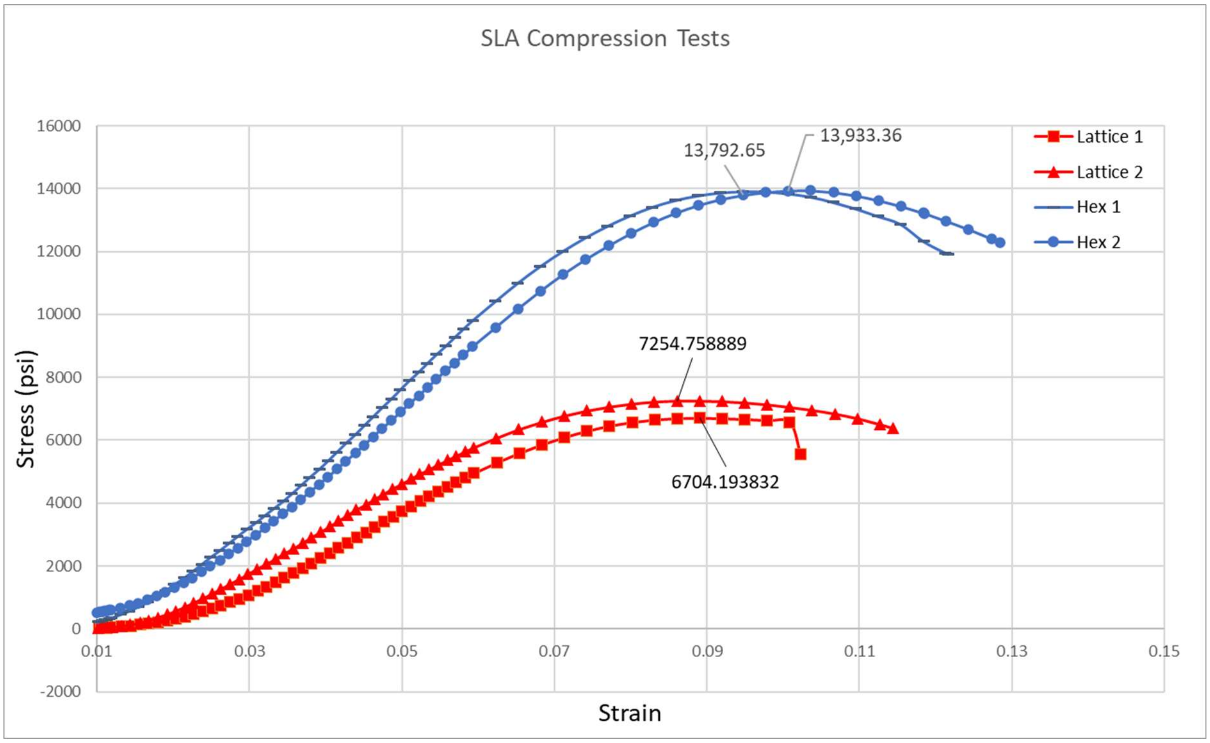

Figure 11: SLA Compression Test Results

Conclusion

This study explores how layer height (LH), infill pattern (IP), and infill density (ID) affect power consumption (PC), surface roughness (SR), and mass for two commonly used AM technologies, SLA and FFF. Results indicate that FFF consumes 4 times more energy than SLA does to fabricate the cubic specimens. SLA is again proven to have superior SR quality. Process parameter values are chosen to be 0.1 mm LH, 10% ID, and honeycomb for IP. These values are chosen due to their effects on response variables.

To validate the process parameter effects, three models are chosen for data collection. The models are chosen based on their different backgrounds and complexities. The three models are: knee joint, steering knuckle, and a bolt. A cubic lattice infill structure is introduced in the validation study, in order to explore its light-weighting capabilities and its PC characteristics.

Validation study data indicates that FFF consumed 8 times more energy with these models. Comparing the two infill structures yielded to the conclusion that SLA responds much better to utilizing the cubic lattice infill. This is due to the larger PC in FFF when fabricating the cubic lattice infill, and due to the negligible weight loss observed in FFF. A mass reduction of 1.5% is seen for FFF models, while SLA sees a 20% mass reduction while maintaining similar PC characteristics if not less.

Acknowledgements

This material is based upon work supported by the National Science Foundation under Grant No. 1801120, "Smart Manufacturing for America's Revolutionizing Technological Transformation". Any opinions, findings, and conclusions or recommendations expressed in this material are those of the author(s) and do not necessarily reflect the views of the National Science Foundation.

References

[1] Hasanov, Seymur. (2021). Numerical Modeling and Experimental Characterization of Functionally Graded Materials Manufactured by the Fused Filament Fabrication Process, Tennessee Tech University. ProQuest Dissertations Publishing, 28646169.

[2] Wong, Kaufui V., and Aldo Hernandez. "A review of additive manufacturing." ISRN Mechanical Engineering. v. 2012. Article ID 208760. (2012).

[3] Kim, G. D., and Y. T. Oh. "A benchmark study on rapid prototyping processes and machines: quantitative comparisons of mechanical properties, accuracy, roughness, speed, and material cost." Proceedings of the Institution of Mechanical Engineers, Part B: Journal of Engineering Manufacture 222.2 (2008): 201-215.

[4] Jayaram, Dureen, et al. "Benchmarking of rapid prototyping systems-Beginning to set standards." 1994 International Solid Freeform Fabrication Symposium. 1994.

[5] Choudhari, C. M., and V. D. Patil. "Product development and its comparative analysis by SLA, SLS and FDM rapid prototyping processes." IOP Conference Series: Materials Science and Engineering. Vol. 149. No. 1. IOP Publishing, 2016.

[6] Terry, S.; Lu, H.; Fidan, I.; Zhang, Y.; Tantawi, K.; Guo, T.; Asiabanpour, B. The Influence of Smart Manufacturing towards Energy Conservation: A Review. Technologies 2020, 8, 31. https://doi.org/10.3390/technologies8020031, accessed on 06/02/2022

[7] Hinshaw, Hunter James, Shane Terry, and Ismail Fidan. "Power consumption investigation for fused filament fabricated specimen." International Journal of Rapid Manufacturing 9.2-3 (2020): 268-279.

[8] Chu, Timothy Scott, et al. "Increasing material efficiency of additive manufacturing through lattice infill pattern." Journal Title 10.1 (2020): 101-108.

[9] Mahesh, Mani, et al. "Benchmarking for decision making in rapid prototyping systems." IEEE International Conference on Automation Science and Engineering, 2005.. IEEE, 2005.

[10] Johnson, Wayne M., et al. "Comparative evaluation of an open-source FDM system." Rapid Prototyping Journal (2014).

[11] Rebaioli, Lara, and Irene Fassi. "A review on benchmark artifacts for evaluating the geometrical performance of additive manufacturing processes." The International Journal of Advanced Manufacturing Technology 93.5 (2017): 2571-2598.

[12] García-Domínguez, Amabel, Juan Claver, and Miguel A. Sebastián. "Infill optimization for pieces obtained by 3D printing." Procedia Manufacturing 41 (2019): 193-199.

[13] Ansys® SpaceClaim, Release 2022R1

[14] Raise3D (2018). Pro 2. https://www.raise3d.com/products/pro2-3d-printer/, accessed on 06/02/2022

[15] Raise3D ideaMaker, Release 4.2.3

[16] Formlabs (2015). Form 2. https://formlabs.com/3d-printers/form-2/, accessed on 06/02/2022

[17] Formlabs Preform, Release 3.24.0

[18] Vernier. Watts Up Pro. https://www.powermeterstore.com/p1206/watts_up_pro.php, accessed on 06/02/2022

[19] Mettler Toledo. PL602-s. https://www.mt.com/my/en/home/products/Laboratory_Weighing_Solutions/Precision_Balances/Standard/PL-E_Precision/PL602E.html, accessed on 06/02/2022

[20] Mitutoyo (2016). SJ-210. https://www.mitutoyo.com/products/form-measurement-machine/surface-roughness/sj-210-portable-surface-roughness-tester-2/

[21] macouno, (2014). Knee Joint [STL]. Thingiverse. https://www.thingiverse.com/thing:234607, accessed on 06/02/2022

[22] Xlnt3D, (2020). Tamiya TL-01 Steering Knuckle [STL]. Thingiverse. https://www.thingiverse.com/thing:4398033, accessed on 06/02/2022

[23] akira3dp0, (2016). Knurling Bolt and Nut [STL]. Thingiverse. https://www.thingiverse.com/thing:1460364, accessed on 06/02/2022